

Supplementary Information

The assembly modules deformation strategy improved the chemical stability and self-assembly stability of docetaxel prodrugs nanoassemblies

Wenjing Wang^{a,1}, Shuo Wang^{a,1}, Shengyao Xu^a, Rong Chai^d, Jun Yuan^a, Hao Zhang^a,
Yaqi Li^a, Xiaohui Pu^c, Xin Li^e, Jin Sun^{a,b}, Zhonggui He ^{a,b,c*}, Bingjun Sun^{a,b*}

Affiliations:

¹Both authors contributed equally to this work.

^a Department of Pharmaceutics, Wuya College of Innovation, Shenyang Pharmaceutical University, Shenyang, 110016, China.

^b Joint International Research Laboratory of Intelligent Drug Delivery Systems, Ministry of Education, China.

^c State Key Laboratory of Antiviral Drugs, School of Pharmacy, Henan University, N. Jinming Ave., Kaifeng 475004, China.

^d Peking Union Second Pharmaceutical Factory Ltd, Beijing 102600, China.

^e Department of Respiratory Disease, The First Affiliated Hospital of Jinzhou Medical University, Jinzhou 121001, China.

*Corresponding author: Prof. Zhonggui He, Ph.D and Prof. Bingjun Sun, Ph.D.

No. 59 Mailbox, Department of Pharmaceutics, Wuya College of Innovation, Shenyang Pharmaceutical University, 103 Wenhua Road, Shenyang 110016, China.

Tel and Fax: +86-024-23986325; E-mail address: hezgui_student@aliyun.com;
sunbingjun_spy@sina.com

Materials

Docetaxel (DTX) was prepared by Ricentik (Hubei, China). Glutathione (GSH), methyl thiazolyl tetrazolium (MTT), trypsin and all culture media were derived from Dalian Meilun Biotechnology Co., Ltd. (Dalian, China). Isostearic acid (IS) was provided by Shanghai Haohong Scientific Co., Ltd. Oleic acid (OA) was prepared by Shanghai Bide Medical Technology Co., Ltd. Hydroxybenzotriazole (HOBT) and *N*-(3-dimethylaminopropyl)-*N'*-ethylcarbodiimide hydrochloride (EDCI) were obtained from Macklin Biochemical Technology Co., Ltd. (Shanghai, China). DSPE-mPEG_{2K} was derived from AVT (Shanghai) Pharmaceutical Tech Co., Ltd. (Shanghai, China). 4-dimethylaminopyridine (DMAP) and coumarin-6 (C-6) were obtained from Shanghai Aladdin Biochemical Technology Co., Ltd. (Shanghai, China). Microtubule Tracker Red detection kit was purchased from Baiolaibo Technology Co., Ltd. (Beijing, China). Annexin V-FITC/PI apoptosis detection kit was supplied by Beijing Solarbio Science & Technology Co., Ltd. (Beijing, China). Culture dishes, plates, and centrifugetubes were purchased from NEST Biotechnology Co., Ltd. (Wuxi, China). All the other reagents and solvents utilized in this study were of analytical grade.

Cell culture

From the cell bank of the Chinese Academy of Sciences (Beijing, China), the L02, 4T1, Lewis, A549, and KB cells. The media, which contained 10% fetal bovine serum (FBS), penicillin (100 units/ml), and streptomycin (100 g/ml) was used to cultivate the cells. At 37 °C, all cells were maintained under a humidified atmosphere of 5% CO₂.

Animal studies

All the animal experiments were approved by the Institutional Animal Ethical Care Committee (IAEC) of Shenyang Pharmaceutical University and in strict accordance with the Guide for the Management and Use of Laboratory Animals.

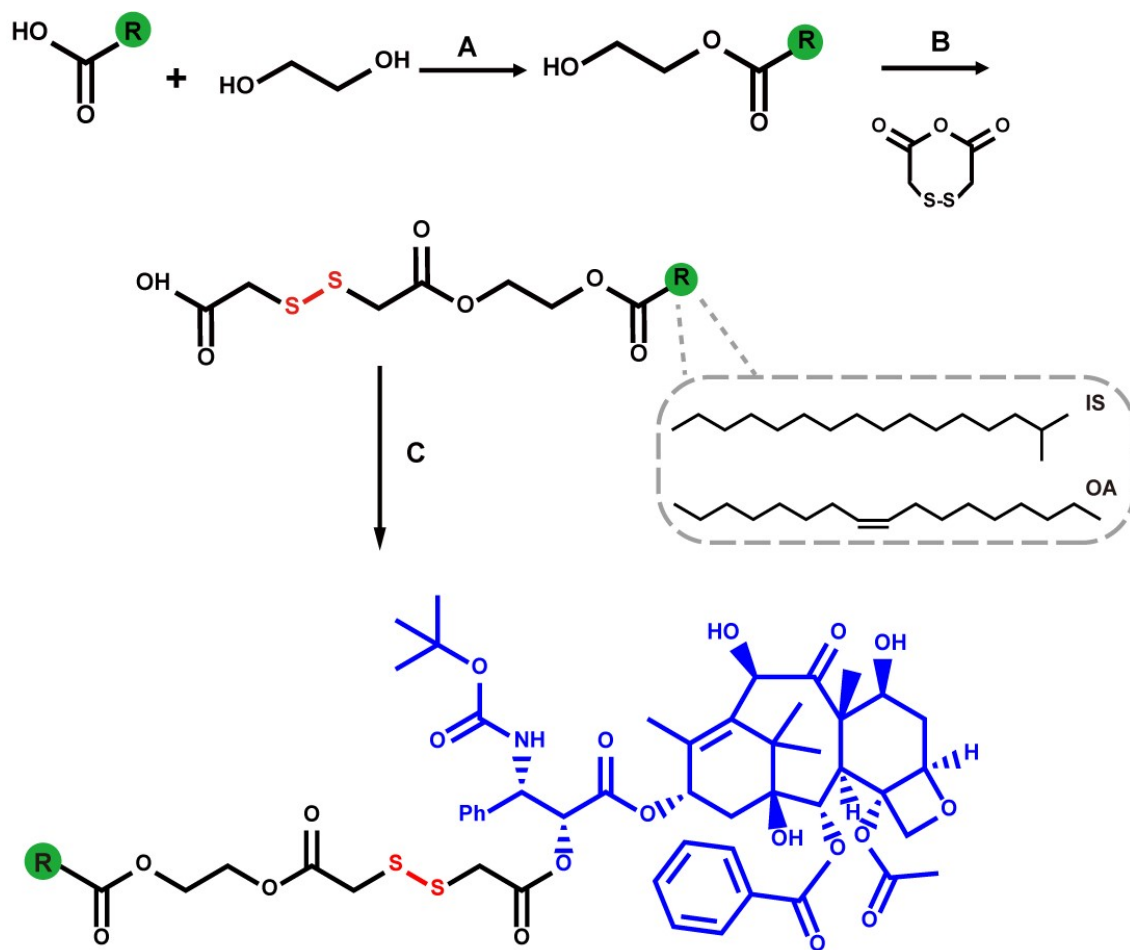


Fig. S1. The synthetic pathways of prodrugs. (A): P-toluenesulfonic acid, 110 °C, 2-3 h; (B): DMAP, 25 °C, 12 h; (C): EDCI, HOBT, DMAP, 0 °C, 2 h; Docetaxel, 25 °C, 36 h.

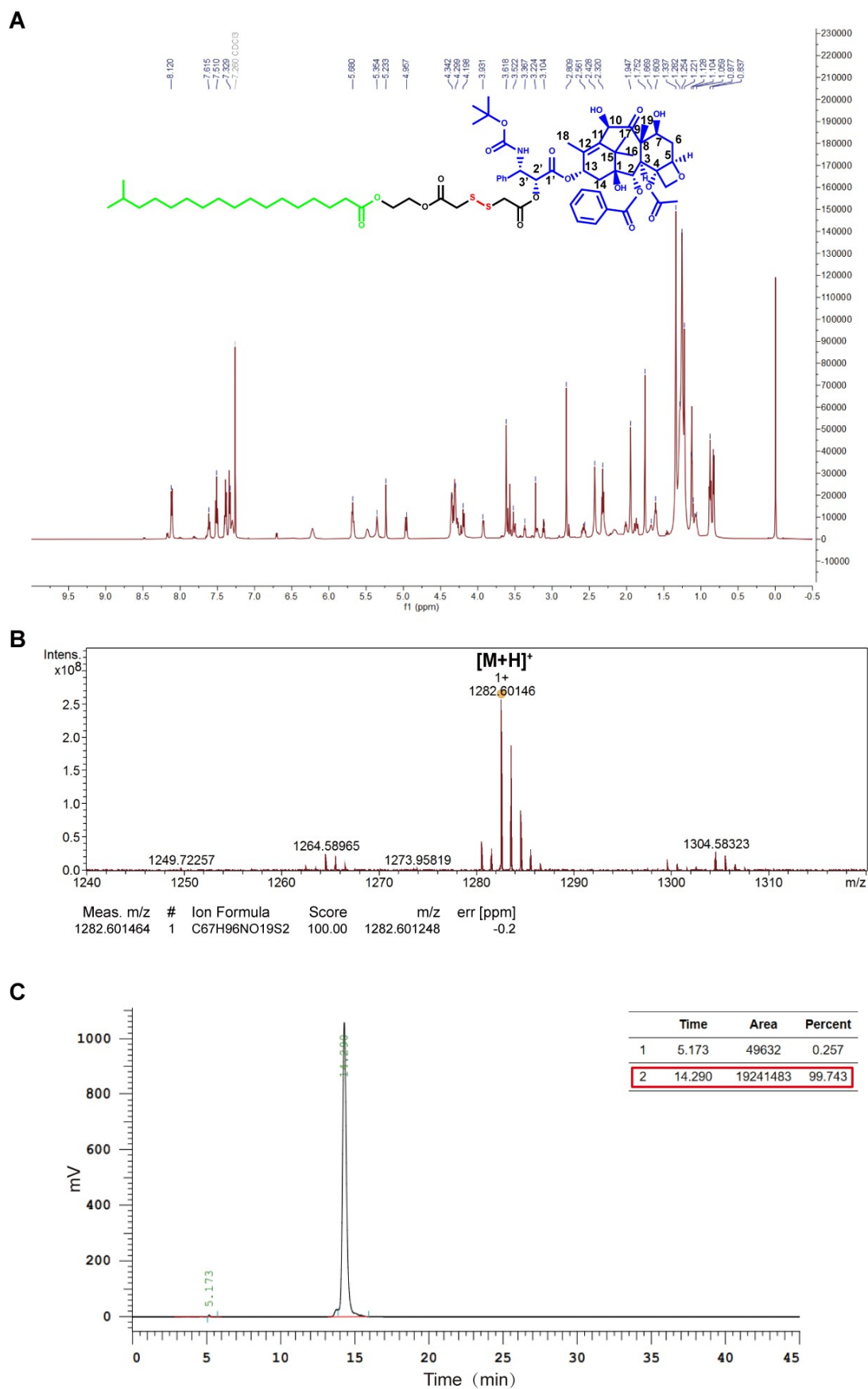


Fig. S2. Characterizations of DTX-SS-IS. (A) ^1H NMR spectrum. (B) Mass spectrum. (C) The purity.

^1H NMR (600 MHz, CDCl_3) δ ppm 8.11 (d, 2H, Ar-H, $J = 7.6$ Hz), 7.61 (t, 1H, Ar-H, $J = 7.5$ Hz), 7.51 (t, 2H, Ar-H, $J = 7.8$ Hz), 7.39 (t, 2H, Ar-H, $J = 7.7$ Hz), 7.33 (d, 2H, Ar-H, $J = 7.4$ Hz), 7.32- 7.28 (m, 1H, Ar-H), 6.22 (s, 1H, 2'-CH), 5.68 (t, 2H, 3'-CH, $J = 7.9$ Hz), 5.49 (s, 1H, 10-CH), 5.23 (s, 1H, 13-CH), 4.96 (dd, 1H, 1-OH, $J = 9.6, 2.3$ Hz), 4.19 (d, 1H, 2-CH, $J = 8.6$ Hz), 3.92 (d, 1H, 5-CH, $J = 7.4$ Hz), 3.59 (d, 4H, CH_2SSCH_2 , $J = 29.6$ Hz), 2.58 (ddd, 1H, 3-CH, $J = 14.4, 9.7, 6.5$ Hz), 2.43 (s, 3H, - CH_2 -H), 1.95 (s, 3H, - CH_3), 1.75 (s, 3H, 18- CH_3), 1.34 (s, 9H, - $(\text{CH}_3)_3$), 1.32-1.16 (m, 31H, - (CH_2) -H,- CH_3), 1.12 (s, 3H, 19- CH_3), 0.89-0.82 (m, 6H, - $(\text{CH}_3)_2$).

HRMS calcd. for $\text{C}_{67}\text{H}_{95}\text{NO}_{19}\text{S}_2$, (ESI) m/z $[\text{M}+\text{H}]^+ = 1282.60146$.

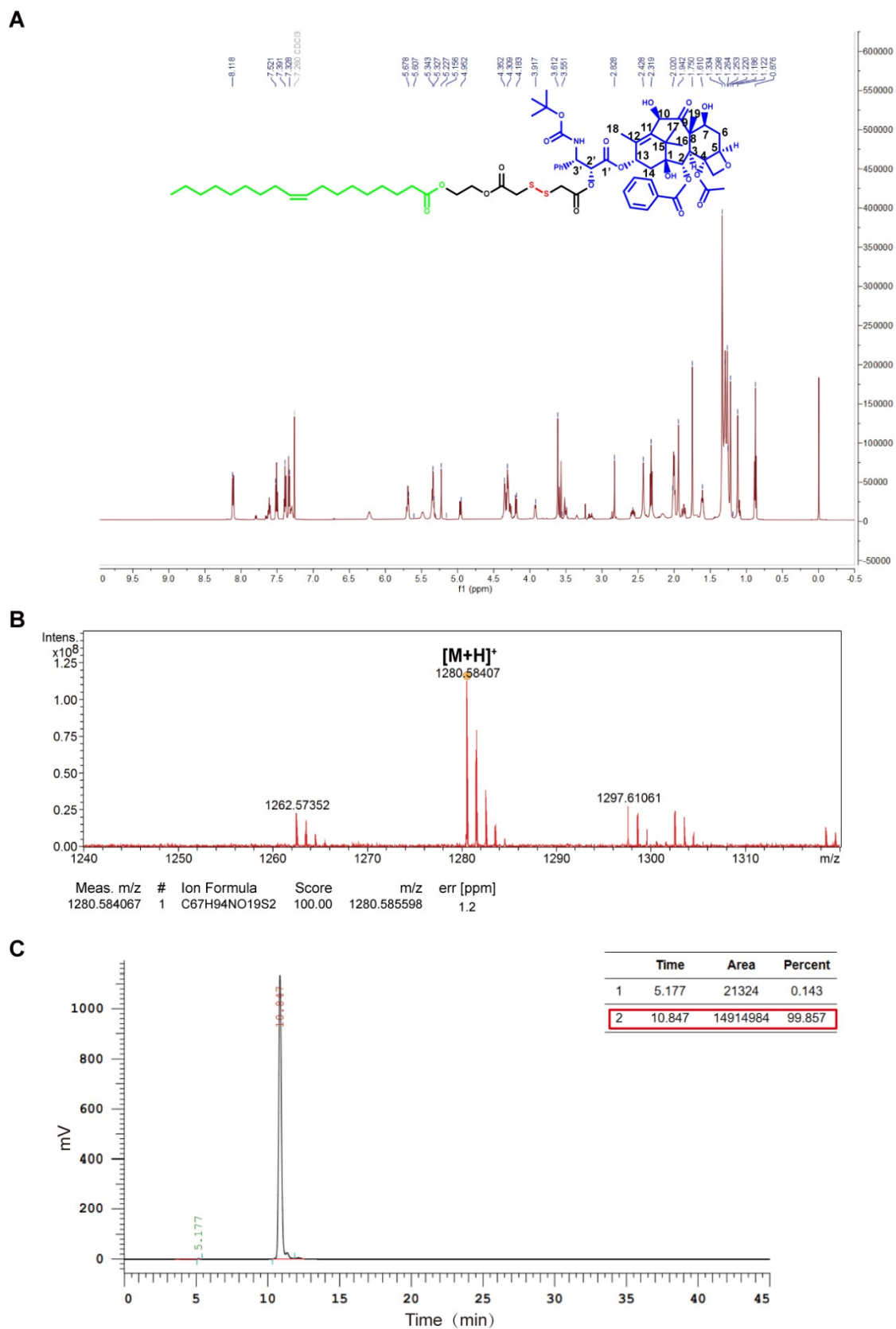


Fig. S3. Characterizations of DTX-SS-OA. (A) ^1H NMR spectrum. (B) Mass spectrum. (C) The purity.

^1H NMR (600 MHz, CDCl_3) δ ppm 8.11 (d, 2H, Ar-H, $J = 7.5$ Hz), 7.61 (t, 1H, Ar-H,

J = 7.4 Hz), 7.51 (t, 2H, Ar-H, J = 7.8 Hz), 7.39 (t, 2H, Ar-H, J = 7.7 Hz), 7.33 (d, 2H, Ar-H, J = 7.4 Hz), 7.30 (t, 1H, Ar-H, J = 7.4 Hz), 6.23 (d, 1H, 2'-CH, J = 9.3 Hz), 5.69 (d, 1H, 3'-CH, J = 8.7 Hz), 5.48 (s, 1H, 10-CH), 5.38-5.30 (m, 3H, -CH=CH-), 5.23 (s, 1H, 13-CH), 4.96 (dd, 1H, 1-OH, J = 9.7, 2.5 Hz), 4.19 (d, 1H, 2-CH, J = 8.5 Hz), 3.92 (d, 1H, 5-CH, J = 7.1 Hz), 3.63-3.49 (m, 4H, -CH₂SSCH₂-), 2.61-2.54 (m, 1H, 3-CH), 2.43 (s, 3H, -COCH₃), 2.32 (d, 2H, -CH₂, J = 7.6 Hz), 1.94 (s, 3H, -CH₃), 1.91-1.80 (m, 2H, 6-CH₂), 1.75 (s, 3H, 18-CH₃), 1.44-1.24 (m, 29H, -C(CH₃)₃-(CH₂)₁₀), 1.12 (s, 3H, 19-CH₃), 0.88 (t, 3H, -CH₂-CH₃, J = 7.0 Hz).

HRMS calcd. for C₆₇H₉₃NO₁₉S₂, (ESI) m/z [M+H]⁺ = 1280.58407.

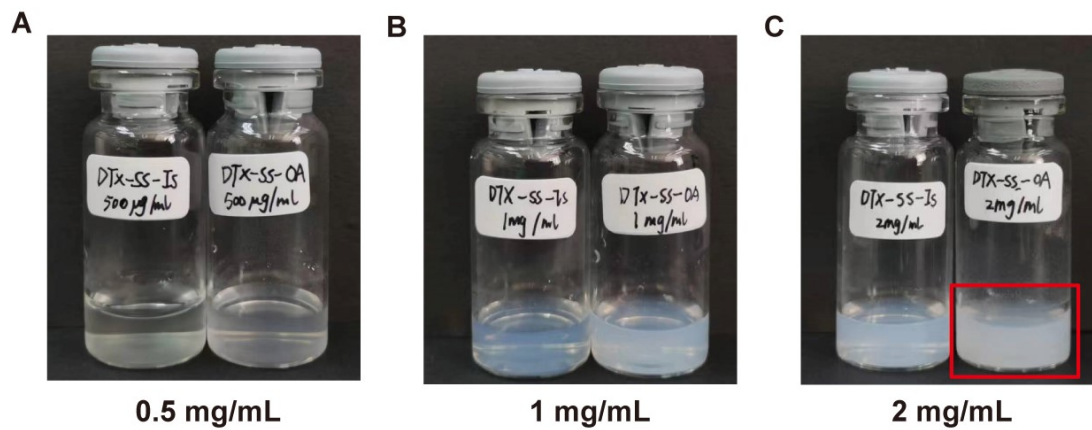


Fig. S4. The appearance of two non-PEGylated DPNs at concentrations of (A) 0.5, (B) 1 and (C) 2 mg/mL.

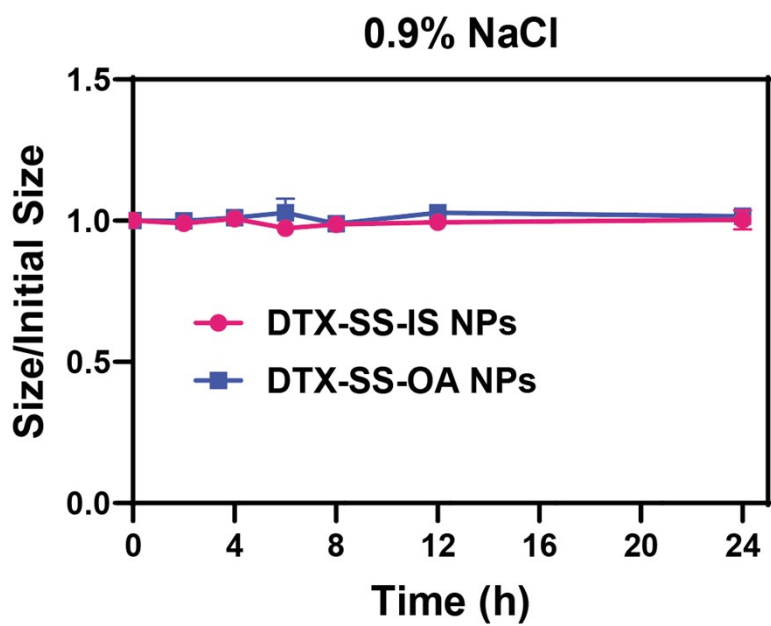


Fig. S5. The stability of PEGylated DPNs in 0.9% NaCl.

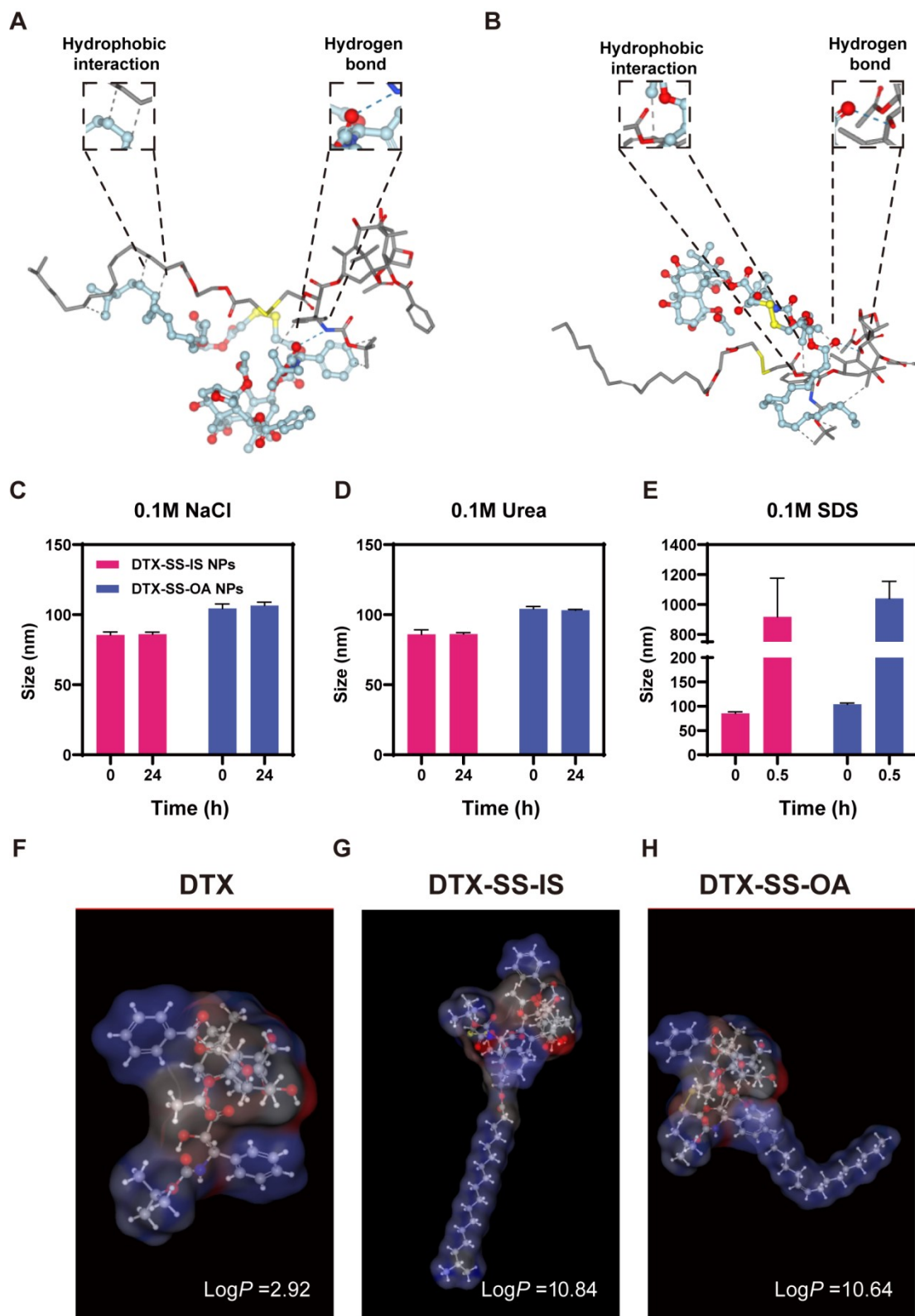


Fig. S6. The optimized geometry structure of DTX-SS-IS (A) and DTX-SS-OA (B). The variation of the particle size of DTX-SS-IS NPs and DTX-SS-OA NPs after co-cubated with (C) NaCl, (D) Urea or (E) SDS. Data are presented as mean \pm SD ($n = 3$). The calculated Log P of (F) DTX, (G) DTX-SS-IS and (H) DTX-SS-OA.

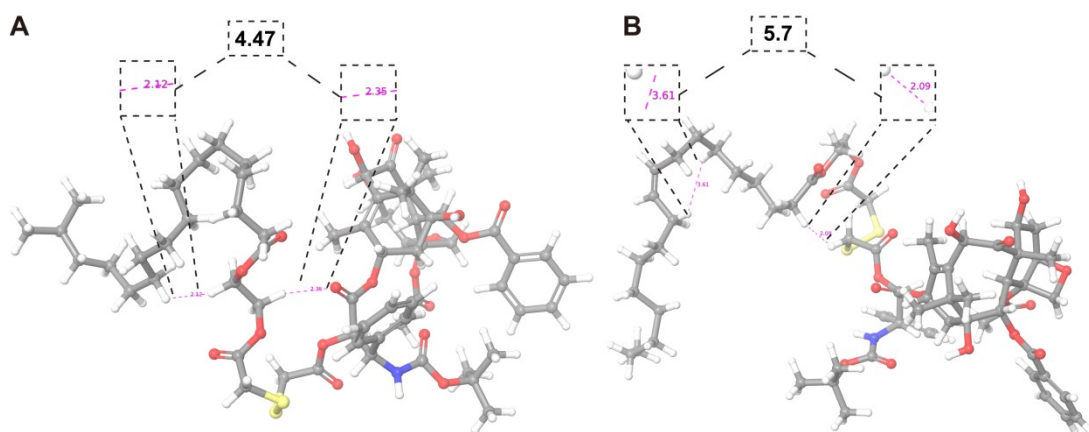


Fig. S7. The steric hindrance analysis of DTX-SS-IS (A) and DTX-SS-OA (B). Steric hindrance caused by interatomic spacing are rendered as pink dashed lines.

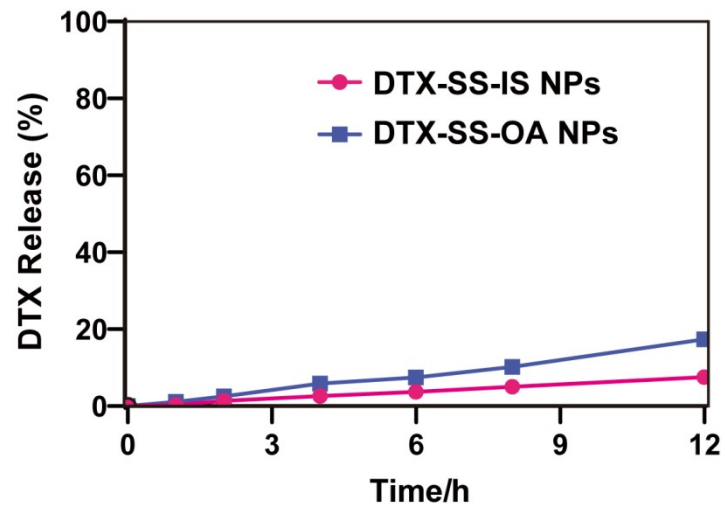


Fig. S8. *In vitro* drug release of DPNs in the medium without redox agents. Data are presented as mean \pm SD (n = 3).

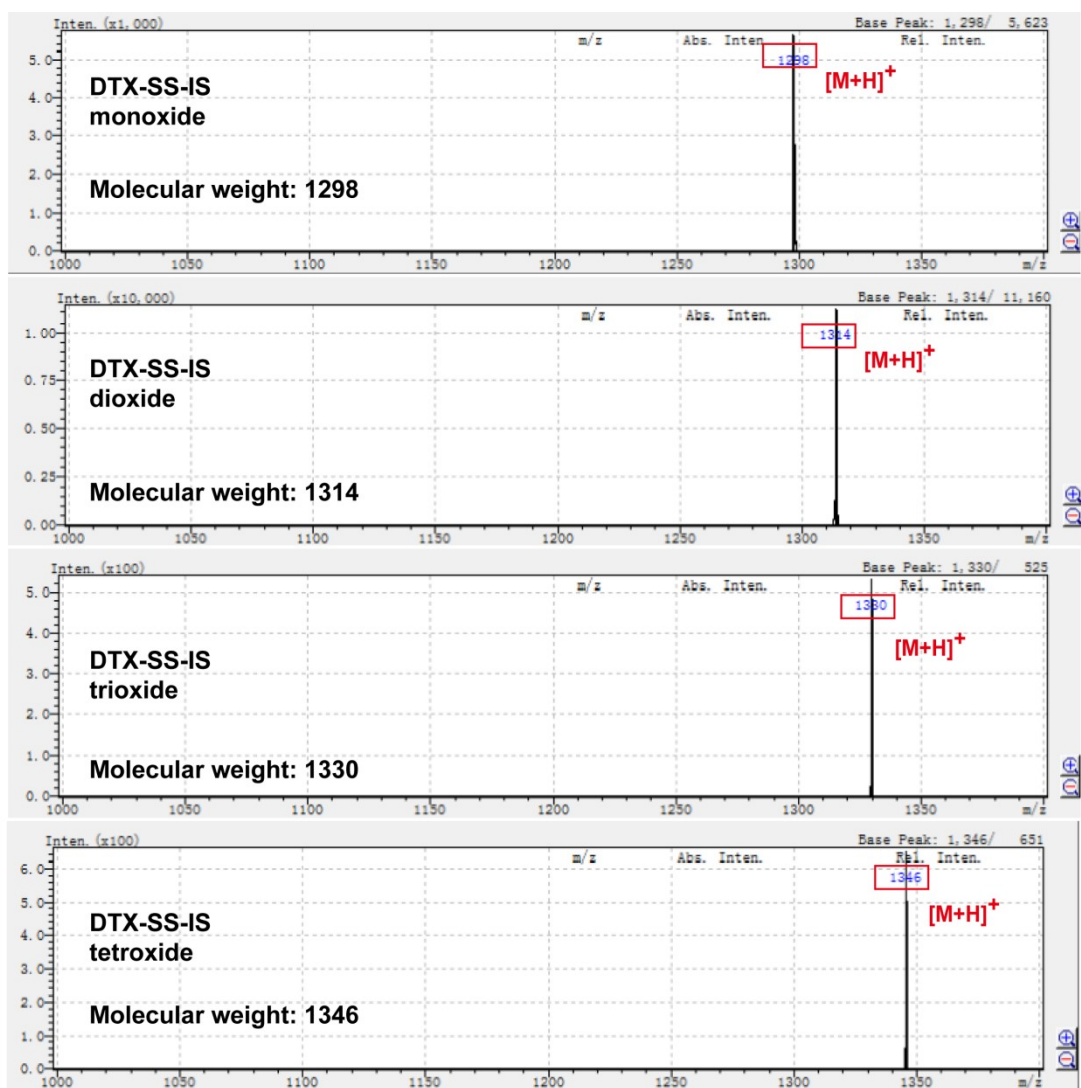


Fig. S9. The oxidation intermediates of DTX-SS-IS NPs.



Fig. S10. The oxidation intermediates of DTX-SS-OA NPs.

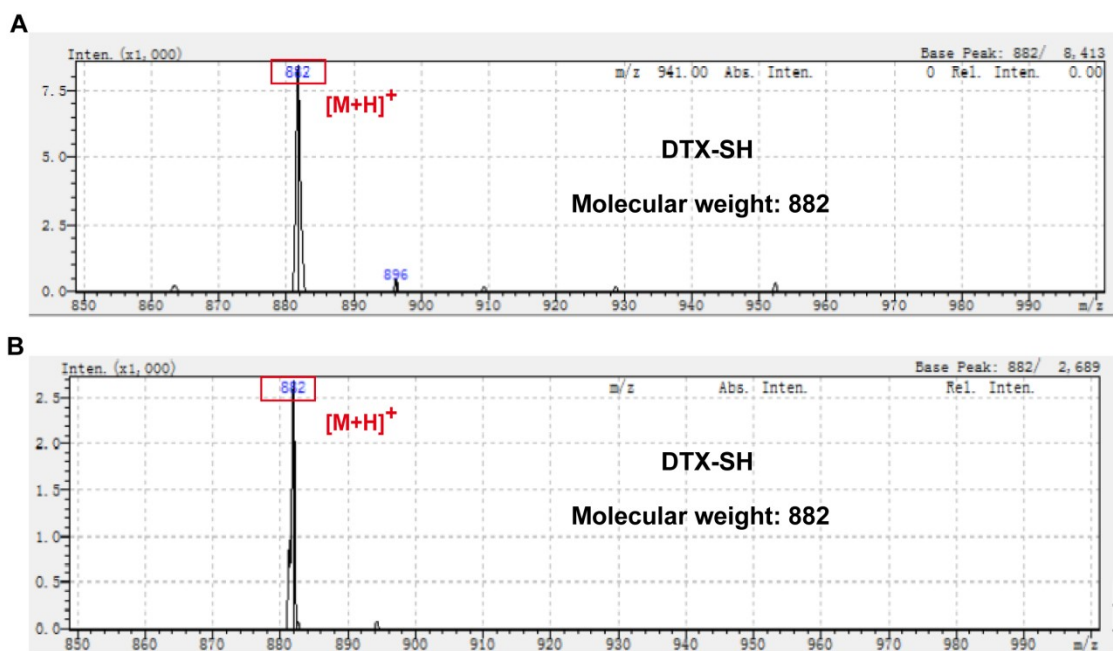


Fig. S11. The reduction intermediates of (A) DTX-SS-IS NPs and (B) DTX-SS-OA NPs

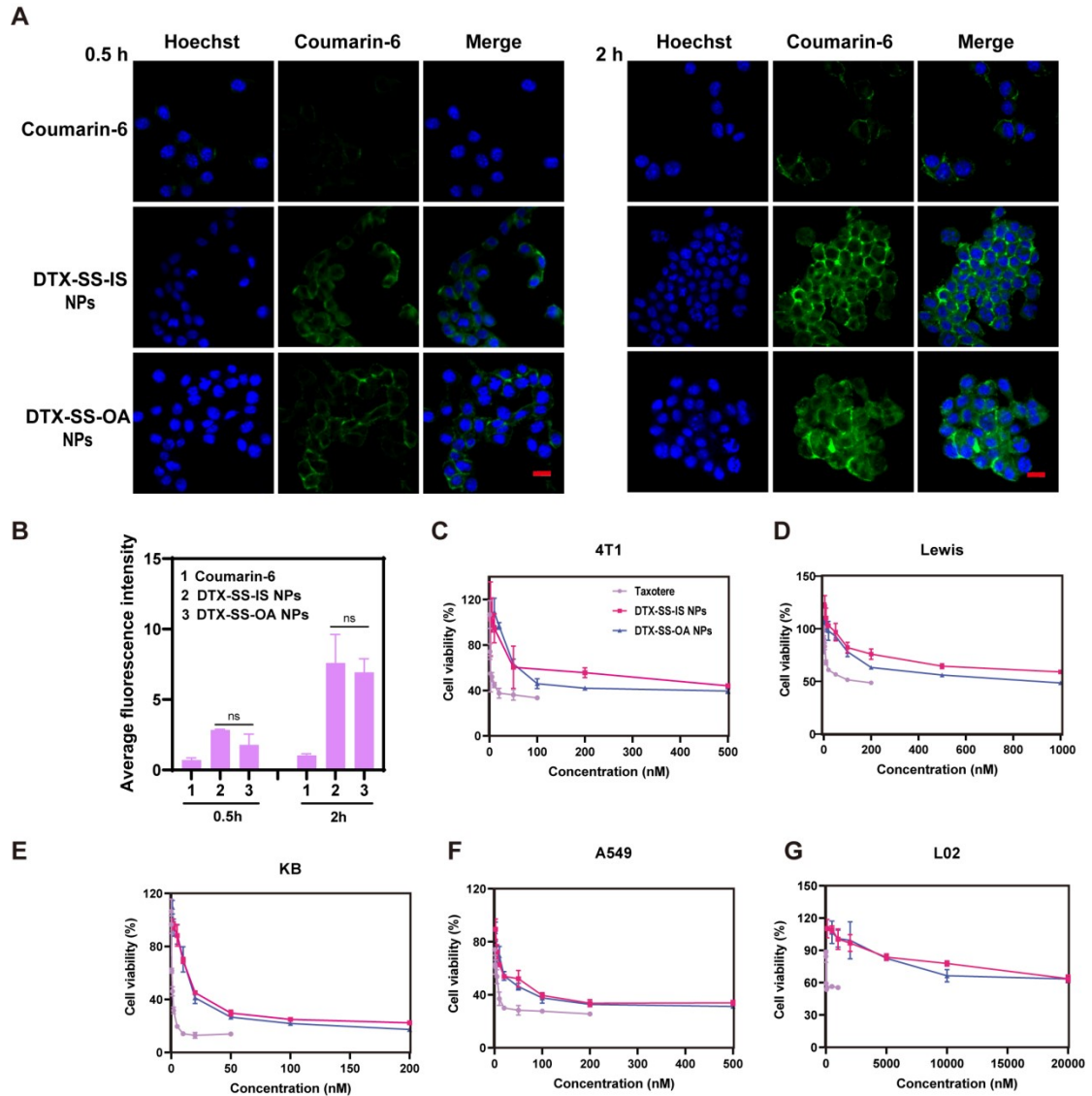


Fig. S12. Cellular uptake of free coumarin-6 or coumarin-6 labeled DPNs at 0.5 h and 2 h (A). Scale bar represents 10 μm . (B) Fluorescence quantitative results of CLSM images at 0.5 h and 2 h. Data are presented as mean \pm SD ($n = 3$). Cell viability treated with various concentrations of Taxotere and DPNs: (C) 4T1 cells, (D) Lewis cells, (E) KB cells, (F) A549 cells, and (G) L02 cells. All data are presented as means \pm SD ($n = 3$) and were analyzed by two-tailed Student's t test using GraphPad Prism 7. $P > 0.05$ (no significance), $*P < 0.05$, $**P < 0.01$, $***P < 0.001$ and $****P < 0.0001$.

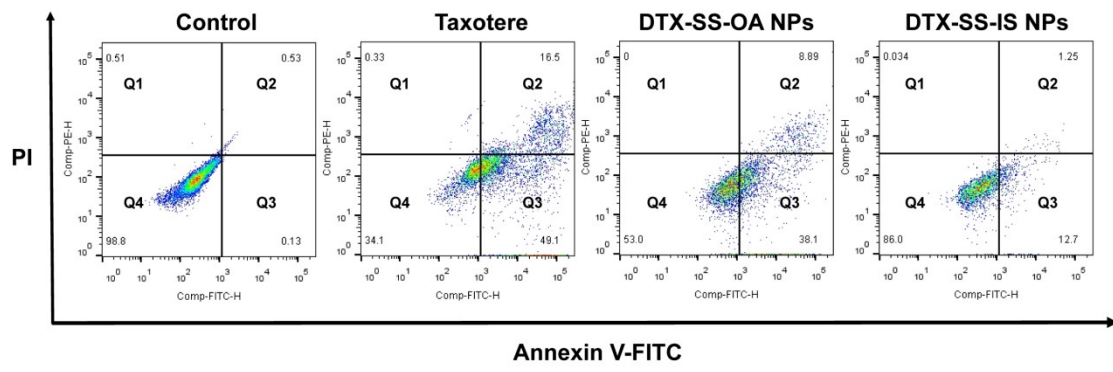


Fig. S13. Cellular apoptosis assay of Taxotere and DPNs in 4T1 cells.

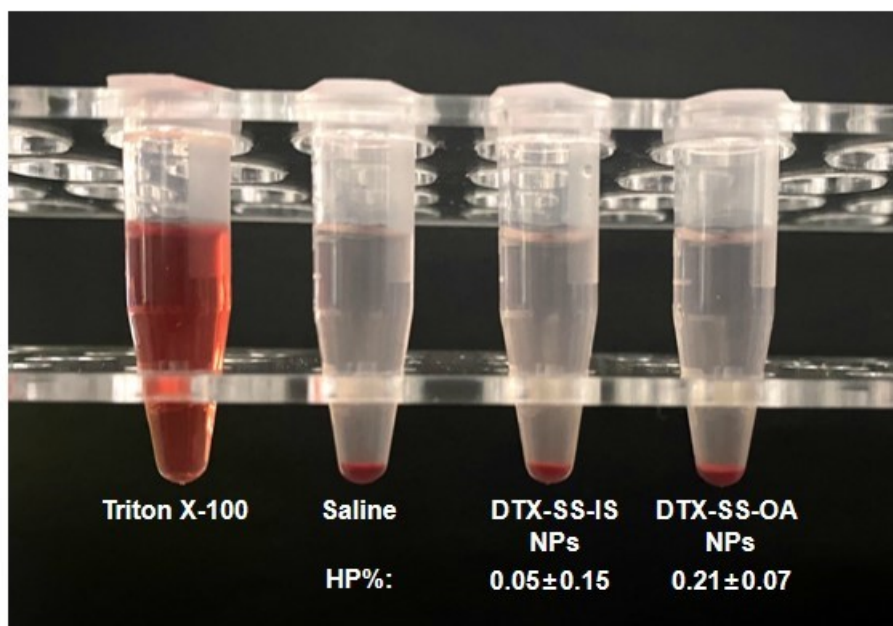


Fig. S14. The hemolysis assay and hemolysis percentage (HP%) of DPNs. The data are presented as means \pm SD (n = 3).

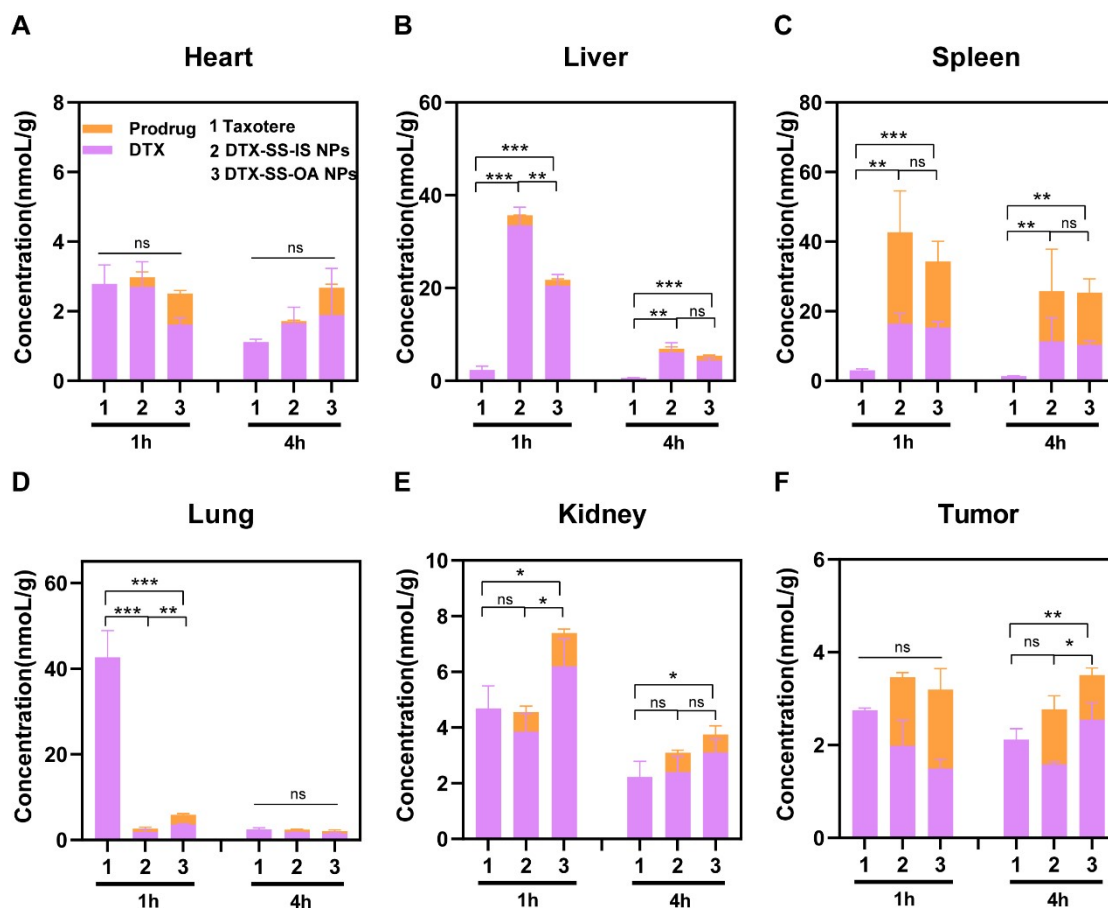


Fig. S15. Biodistribution of PEGylated DPNs in (A) heart, (B) liver, (C) spleen, (D) lung, (E) kidney and (F) tumor. Data are presented as mean \pm SD ($n = 3$). n.s. (no significance) $P > 0.05$, * $P < 0.05$, ** $P < 0.01$, *** $P < 0.001$, and **** $P < 0.0001$ by two-tailed Student's t test.

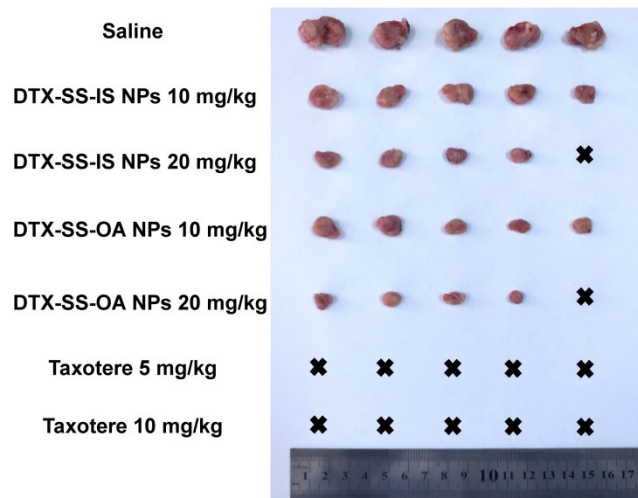
A**B**

Fig. S16. *In vivo* antitumor efficacy of DPNs against (A) 4T1 xenograft tumors (n=5) with cumulative toxicity reflected in the ears of mice (B).

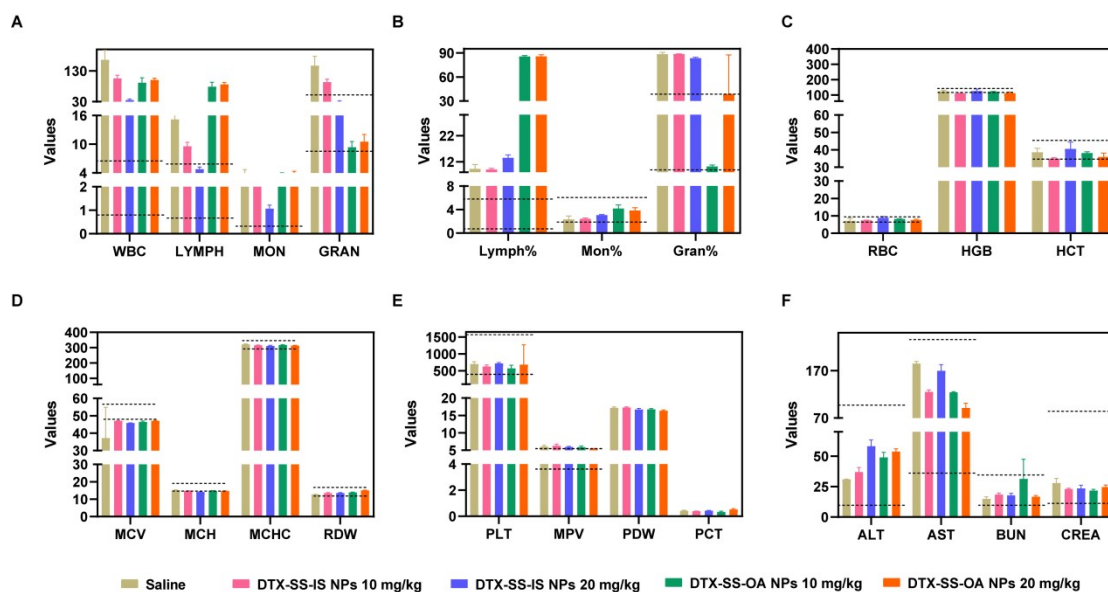


Fig. S17. Safety analysis of DPNs and complete blood count for 4T1 tumor bearing mice. (A) WBC: white blood cell count (10^9 L^{-1}), Lymph: lymphocyte count (10^9 L^{-1}), Mon: monocyte count (10^9 L^{-1}), Gran: granulocyte count (10^9 L^{-1}). (B) Complete blood count for 4T1 tumor bearing mice ($n=3$). Lymph%: lymphocyte percentage (%), Mon%: monocyte percentage (%), Gran%: granulocyte percentage (%). (C) RBC: red blood cell count (10^{12} L^{-1}), HGB: heoglobin (g/L), HCT: hematocrit (%). (D) MCV: mean red blood cell volume (fL), MCH: mean corpuscular hemoglobin (pg), MCHC: mean corpuscular hemoglobin concentration (g/L), RDW: red cell distribution width (%). (E) PLT: platelet count (10^9 L^{-1}), MPV: average platelet volume (fL), PDW: platelet distribution width, PCT: platelet hematocrit (%). (F) ALT: alanine aminotransferase (U/L), AST: aspartate aminotransferase (U/L), BUN: blood urea nitrogen (mmol/L), CREA: creatinine ($\mu\text{mol/L}$). Data are presented as mean \pm SD ($n = 3$).

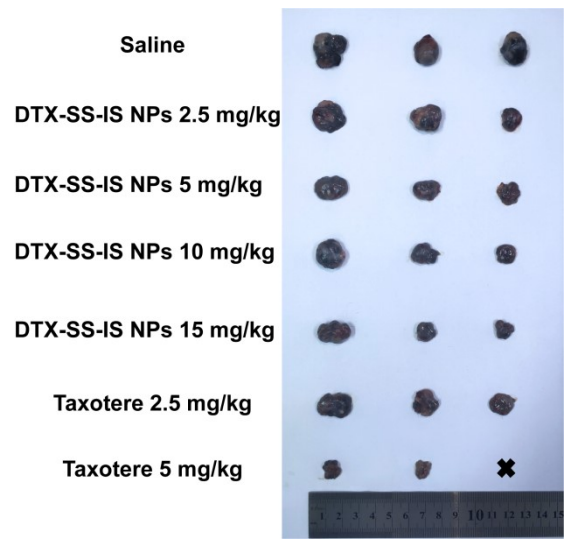


Fig. S18. *In vivo* antitumor efficacy of DPNs against Lewis xenograft tumors (n=3).

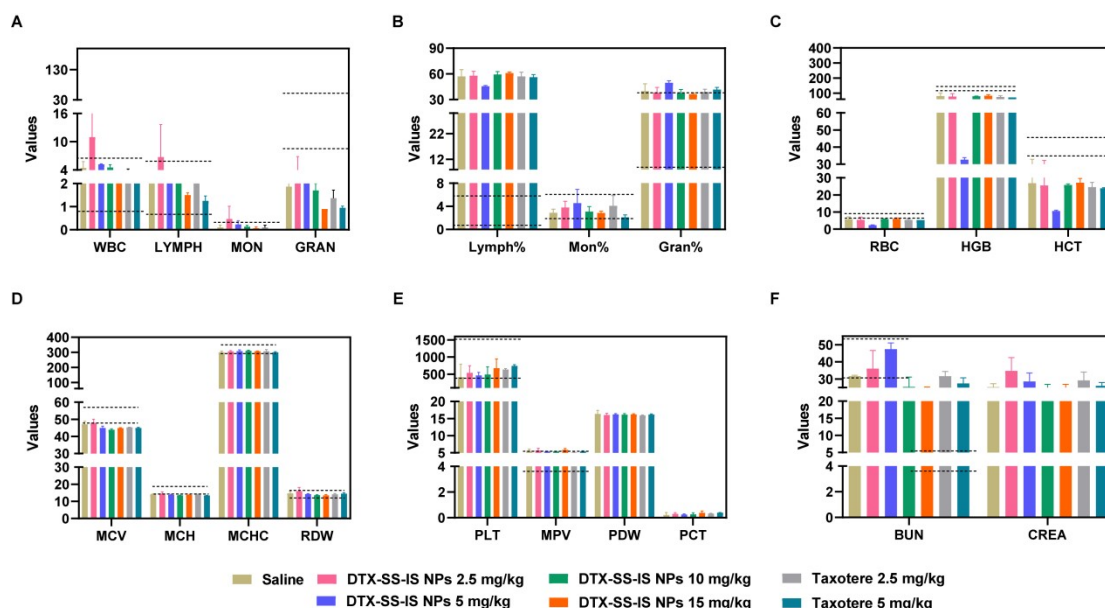


Fig. S19. Safety analysis of DPNs and complete blood count for Lewis tumor bearing mice. (A) WBC: white blood cell count ($10^9 L^{-1}$), Lymph: lymphocyte count ($10^9 L^{-1}$), Mon: monocyte count ($10^9 L^{-1}$), Gran: granulocyte count ($10^9 L^{-1}$). (B) Complete blood count for Lewis tumor bearing mice ($n=3$). Lymph%: lymphocyte percentage (%), Mon%: monocyte percentage (%), Gran%: granulocyte percentage (%). (C) RBC: red blood cell count ($10^{12} L^{-1}$), HGB: heoglobin (g/L), HCT: hematocrit (%). (D) MCV: mean red blood cell volume (fL), MCH: mean corpuscular hemoglobin (pg), MCHC: mean corpuscular hemoglobin concentration (g/L), RDW: red cell distribution width (%). (E) PLT: platelet count ($10^9 L^{-1}$), MPV: average platelet volume (fL), PDW: platelet distribution width, PCT: platelet hematocrit (%). (F) BUN: blood urea nitrogen (mmol/L), CREA: creatinine ($\mu\text{mol/L}$). Data are presented as mean \pm SD ($n = 3$).

Table

Table S1. The particle sizes of non-PEGylated DPNs.

Concentration	DTX-SS-IS NPs	DTX-SS-OA NPs
0.5 mg/mL	84.65 ± 0.31	78.36 ± 2.28
1 mg/mL	110.90 ± 2.17	108.30 ± 4.16
2 mg/mL	133.90 ± 1.00	Obvious precipitation

DPNs, DTX prodrugs nanoassemblies; NPs, nanoassemblies.

Data are presented as mean ± SD (n = 3).

Table S2. Characterization of PEGylated DPNs.

Nanoassemblies	Size (nm)	PDI	Zeta potential (mV)	Drug loading (w/w, %)
DTX-SS-IS NPs	78.85 ± 0.68	0.11 ± 0.06	-20.9 ± 0.67	63.04
DTX-SS-OA NPs	97.16 ± 2.44	0.10 ± 0.07	-29.9 ± 0.76	63.14

DPNs, DTX prodrugs nanoassemblies; NPs, nanoassemblies.

Data are presented as mean ± SD (n = 3).

Table S3. The HPLC conditions for determination of redox dual-sensitive drug release.

Chromatographic column	Column temperature	Detection wavelength	Mobile phase Acetonitrile: water (%)	Velocity of flow (mL/min)
Welch AQ-C18	25 ± 5°C	227 nm	60 : 40	1

Table S4. IC50 values (nmol/L) of Taxotere and DPNs against four tumor cell lines and one normal cell line.

Cell lines	Taxotere	DTX-SS-IS NPs	DTX-SS-OA NPs
4T1	9.622 ± 3.17	346.3 ± 58.42	175.6 ± 24.29
Lewis	106.5 ± 6.87	1157 ± 140.43	694.2 ± 23.95
KB	1.006 ± 0.03	24.33 ± 0.67	21.37 ± 0.09
A549	4.957 ± 0.06	54.53 ± 7.41	48.15 ± 9.68
L02	814.5 ± 149.61	31328 ± 3521.24	27423 ± 6486.64

DPNs, DTX prodrugs nanoassemblies; NPs, nanoassemblies.

Data are presented as mean ± SD (n = 3).

Table S5. The tumor selectivity index (TSI) of Taxotere and DPNs between L02 cells and tumor cells.

Cell lines	Taxotere	DTX-SS-IS NPs	DTX-SS-OA NPs
4T1	84.65	90.46	156.17
Lewis	7.65	27.08	39.50
KB	809.64	1287.63	1283.25
A549	164.31	574.51	569.53

$TSI = (IC_{50normal}) / (IC_{50tumor})$. (“ $IC_{50 normal}$ and $IC_{50 tumor}$ ” represent the IC_{50} of Taxotere or DPNs toward L02 normal cells and tumor cells).

DPNs, DTX prodrugs nanoassemblies; NPs, nanoassemblies.

Table S6. The HPLC conditions for determination of plasma stability.

Time (min)	Acetonitrile (%)	Water (%)
0	60	40
8.0	60	40
8.1	100	0
28.0	100	0
30.0	60	40
33.0	60	40

Table S7. The scanning conditions of UPLC-MS-MS.

Compounds	Parent (m/z)	Daughter (m/z)	Cone (V)	Collision (V)
PTX	876.6	308.2	72	32
DTX	830.5	304.1	57	35
DTX-SS-IS	1305.0	778.2	50	32
DTX-SS-OA	1303.1	776.7	50	28

Table S8. The chromatographic conditions of UPLC-MS-MS.

Chromatographic column	Organic phase (100%)	Velocity of flow (mL/min)	Injection volume (μL)
Phenomenex Kinetex® XB-C18 column	Acetonitrile	0.2	5

Table S9. Pharmacokinetic profiles of Taxotere and DPNs.

Formulations	Determined	AUC_{0-24 h} (nmol*h/mL)	MRT (h)	C_{max} (nmol/mL)
Taxotere	DTX	0.502 ± 0.04	0.420 ± 0.19	3.411 ± 0.43
DTX-SS-IS NPs	DTX-SS-IS	18.784 ± 5.89	0.341 ± 0.03	42.155 ± 15.47
	DTX	15.266 ± 7.38	1.563 ± 0.34	18.484 ± 6.72
DTX-SS-OA NPs	DTX-SS-OA	13.068 ± 5.50	0.303 ± 0.14	38.032 ± 13.79
	DTX	10.719 ± 3.78	1.214 ± 0.20	23.846 ± 12.60

DPNs, DTX prodrugs nanoassemblies; NPs, nanoassemblies.

Data are presented as mean ± SD (n = 3).